International Journal of
INTELLIGENT SYSTEMS AND APPLICATIONS IN ENGINEERING
ISSN:2147-6799 www.ijisae.org Original Research Paper

Enhanced Isolation with and without Stub and T-StubMicrostrip Antenna

Rahul Umesh Kale[1*], Dr. Manish Dhananjay Sawale[2]

Submitted: 08/01/2024 **Revised**: 14/02/2024 **Accepted**: 22/02/2024

Abstract: Microstrip antenna with MIMO technology is used to achieve a high transmission rate for 5G operations below 6 GHz. A filter-based decoupled network has been devised to enhance the isolation among the antenna ports within the MIMO system. In this work, MIMO antenna is designed with and without stub. In addition, the T-stub antenna is also designed. The designed antennas simulated the performance of the same is analyzed via different performance measures. Different performance metrics include S-parameters, radiation properties, mutual coupling and bandwidth. The designed antenna shows a good performance in terms of the mentioned metrics. The design and effectiveness of filter based decoupled network is improving the Isolation fabricate on FR-4 substrate. The simulation result shows that low envelope correction coefficient (ECC≤0.0005) and low mutual coupling (S12≤29). The mentioned three types of antennas are designed using software and their performance is analyzed.

Keywords: *Isolation, Multiple Input Multiple Output (MIMO), Stub, T-Stub*

1. Introduction:

Multi-input-multiple-output (MIMO) antenna systems necessitate spacing between antenna elements to achieve spatial diversity. However, to address the spatial constraints, an alternative approach involves employing filter-based decoupled networks to enhance isolation among the antenna ports in MIMO systems.

Various techniques have been devised to mitigate mutual coupling among closely spaced antenna elements. For instance, artificial magnetic materials were engineered to attenuate electromagnetic coupling [1]. Additionally, low mutual coupling can be attained through electromagnetic band-gap (EBG) structures, which suppress surface waves [2]. Another method involves reducing mutual coupling by approximately 5.5 dB using a series of metal-filled vias to confine resonant modes within the structure [3].

Stub microstrip antennas are a type of planar antenna that utilizes a stub (short length of conductor) to enhance its performance and characteristics. The combination of compact size, low profile, ease of fabrication, and versatility makes microstrip antennas a popular choice for various wireless communication systems. It typically has a narrow strip of conductive material, such as copper, which is connected to the main patch of the microstrip antenna.

A stub microstrip antenna comprises a radiating patch, typically a metallic strip, positioned on one side of a dielectric substrate. This patch is commonly fed using either a coaxial cable or a microstrip transmission line, connected to a designated feed point on the patch. Additionally, a stub—a brief extension of the patch—is linked at a particular juncture along the length of the patch. [15].

An AT-stub microstrip antenna represents a particular arrangement of a stub microstrip antenna, featuring a T-shaped stub. This T-shaped stub typically connects to the radiating patch via a slender feedline. The T-stub assumes a pivotal role in enhancing the impedance matching of the microstrip antenna. Fine-tuning the length and positioning of the T-stub facilitates optimization of antenna performance. The antenna's impedance can be tuned to match the desired value, leading to better performance and reduced reflection losses. T-stub microstrip antennas are commonly used in wireless communication systems, where impedance matching is critical for efficient power transfer between the antenna and the transmission line [4].

Both stub microstrip antennas and T-stub microstrip antennas offer advantages in terms of compact size, ease of fabrication, and tunability of performance parameters. However, their specific characteristics and performance depend on the design, dimensions, and operating frequency of the antenna.

2. Simulated Results of Wideband MIMO antenna without stub

2.1 Design Consideration

The depicted MIMO antenna design, as illustrated in Figure 1, does not incorporate a stub. It presents a novel top view configuration, featuring a semi-circular radiator and a partially constructed step ground plane. The diversity antenna consists of two separate antenna elements positioned 10mm apart along the y-axis.

[1] *Ph.D., Scholar, Oriental University, Indore (M.P.), India*

[2] *Professor, Department of E & TC Engineering, Oriental University, Indore (M.P.), IndiaEmail: prahulkale17@gmail.com*

Fabricated on an FR4 substrate with a relative dielectric constant of 4.4 and a thickness of 1.6mm, the wideband MIMO antenna, excluding the stub, exhibits a remarkably compact size of 40 × 21 mm.

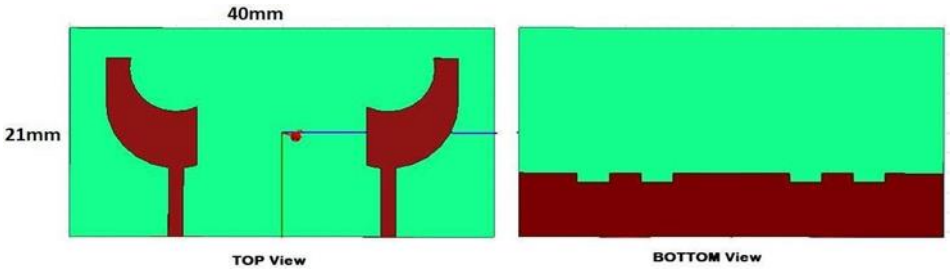

Fig 1. Wideband MIMO antenna without stub

2.1 Results and Discussion

2.2.1 S-Parameters

The S Parameters plot provided demonstrates the performance of the MIMO antenna without a stub. At a resonance frequency of 5.14 GHz, the Return Loss value is recorded at -19.84 dB. In practical terms, an ideal Return Loss value covers around -10 dB, indicating that roughly 90% of the power is directed towards the source while 10% is reflected towards the load. Figure 2 depicts the simulated S11 and S22 parameters of the optimized MIMO element antenna.

Fig 2. Simulated S-Parameters of MIMO antenna without stub

2.2.2 VSWR

Figure 3 presents the VSWR graph, showcasing the performance of the MIMO antenna without a stub. The VSWR value for this antenna remains within the typical range of 1 to 2, meeting established standards. Specifically, at a frequency of 5.47 GHz, the VSWR of the MIMO antenna lacking a stub is measured at 1.07, indicating exceptional impedance. matching and minimal signal reflection.

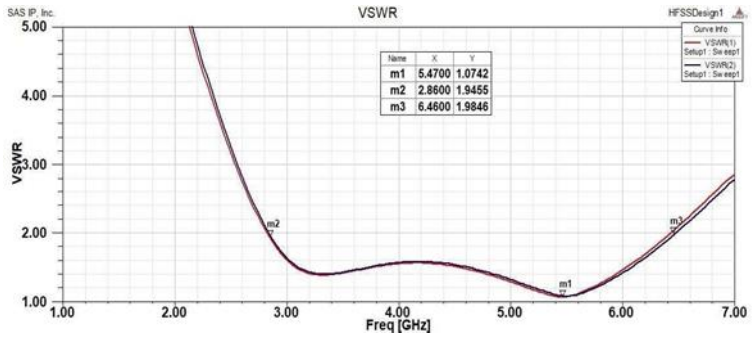

Fig 3. Simulated VSWR of MIMO antenna without stub

2.2.3 Isolation Graph (S21):

Figure 4 depicts the isolation S21 plot, which illustrates the performance attributes of the MIMO antenna when a stub is not utilized. Notably, the plot indicates that the isolation (S21) consistently stays below -15.00 dB throughout the entire operational bandwidth. This indicates successful suppression of undesired coupling between antenna elements, guaranteeing dependable performance within the designated frequency range.

Fig 4. Isolation S21 of MIMO Antenna without stub

2.2.4 Radiation Pattern graph (2D & 3D)

Figure 5 depicts the radiation pattern of the MIMO antenna in the absence of a stub, showcased at a frequency of 3.5 GHz. Subfigure (a) portrays the antenna's radiation pattern without a stub, depicted as bi-directional in the E-plane (shown in blue) and omnidirectional in the H-plane (represented in red). Subfigure (b) demonstrates that the maximum gain of the antenna, highlighted in red, reaches approximately 2.0 dB at 3.5 GHz. This highlights the directional characteristics of the antenna's radiation pattern and its capability to achieve substantial gain at the designated frequency.

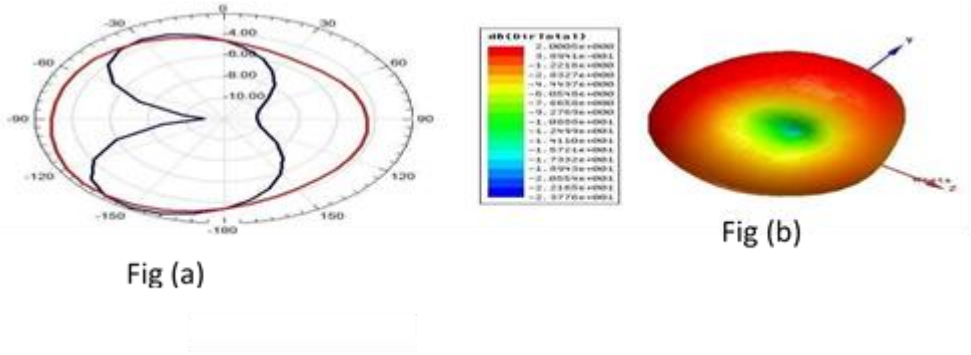

Fig 5. Simulated radiation pattern and gain for the MIMO antenna lacking a stub.

3. Simulated Results of Wideband MIMO Antenna with Stub

3.1 Design Consideration

Figure 6 depicts the configuration of the suggested MIMO antenna setup featuring a stub. The top-down view of this MIMO diversity antenna exhibits a semi-circular radiator coupled with a stepped partial ground plane. Noteworthy is that the diversity antenna consists of two antenna elements placed 10 mm apart along the y-axis. This distinctive layout enables improved diversity performance, enabling efficient signal reception and transmission across different conditions.

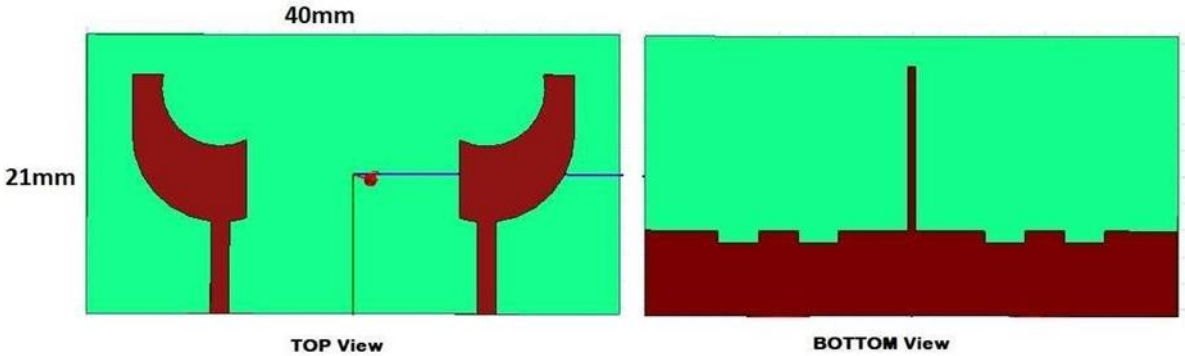

Fig 6. Wideband MIMO antenna with stub

3.2 Results and Discussion

3.2.1 S-Parameters graph

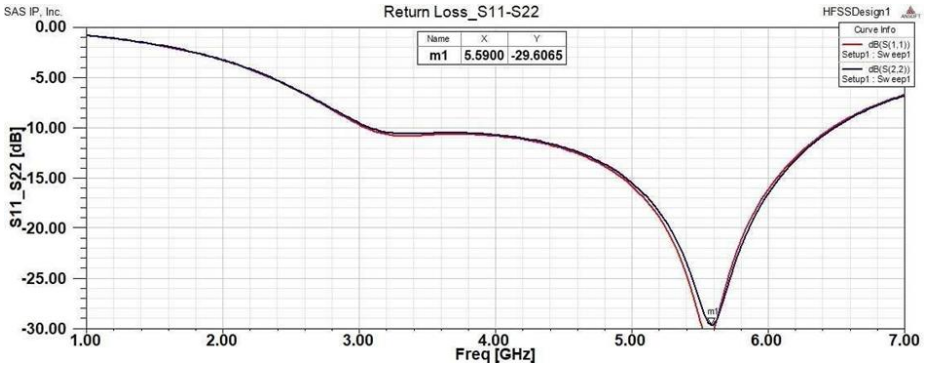

Fig 7. Simulated S-Parameters of MIMO antenna with stub

The S Parameters plot provided illustrates the performance of the MIMO antenna incorporating a stub. It's important to note that the resonance frequency of this antenna is detected at 5.59 GHz. Furthermore, the simulated S11 and S22 parameters of the refined MIMO element antenna are presented alongside Figure 7. Examination of the return loss of the MIMO antenna featuring a stub indicates a reading of -29.60 dB at 5.14 GHz, suggesting excellent impedance matching and negligible signal reflection.

3.2.2 VSWR graph

Displayed in Figure 8 is the VSWR graph illustrating the performance of the MIMO antenna incorporating a stub. Notably, the VSWR value for this antenna falls within the accepted range of 1 to 2, meeting standard requirements. Specifically, at a frequency of 5.53 GHz, the VSWR of the MIMO antenna with a stub registers at 1.06, indicating excellent impedance matching and optimal signal transmission.

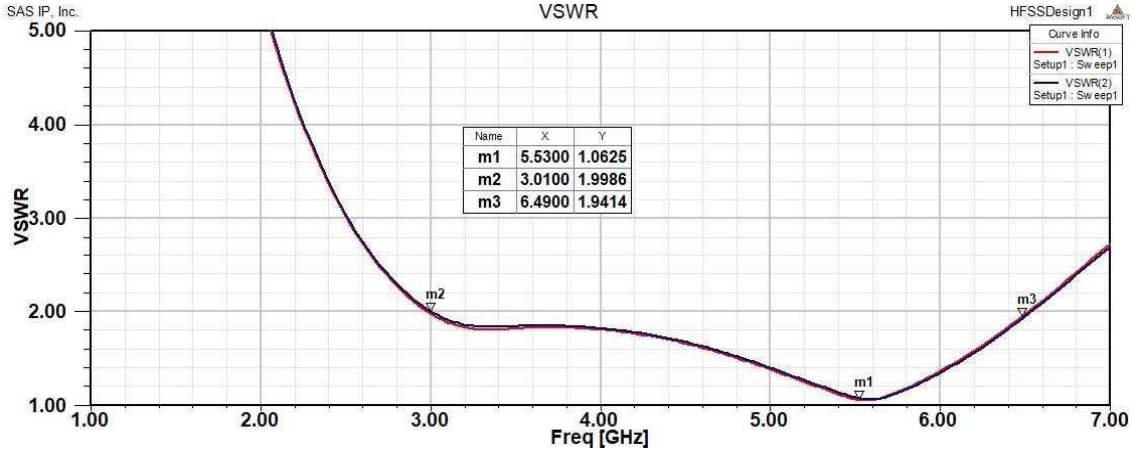

Fig 8. Simulated VSWR of MIMO antenna with stub

3.2.3 Isolation Graph (S21)

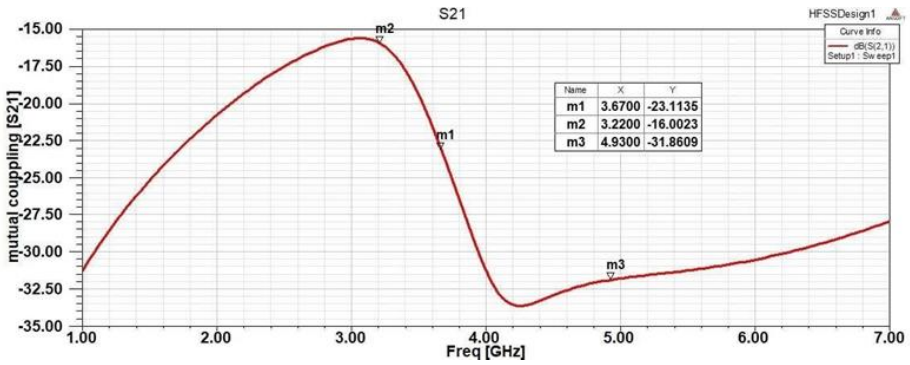

Fig 9. Isolation S21 of MIMO Antenna with stub

Figure 9, which depicts the isolation (S21) of the MIMO antenna featuring a stub, shows that it consistently stays under -16.00 dB throughout the operational frequency range.

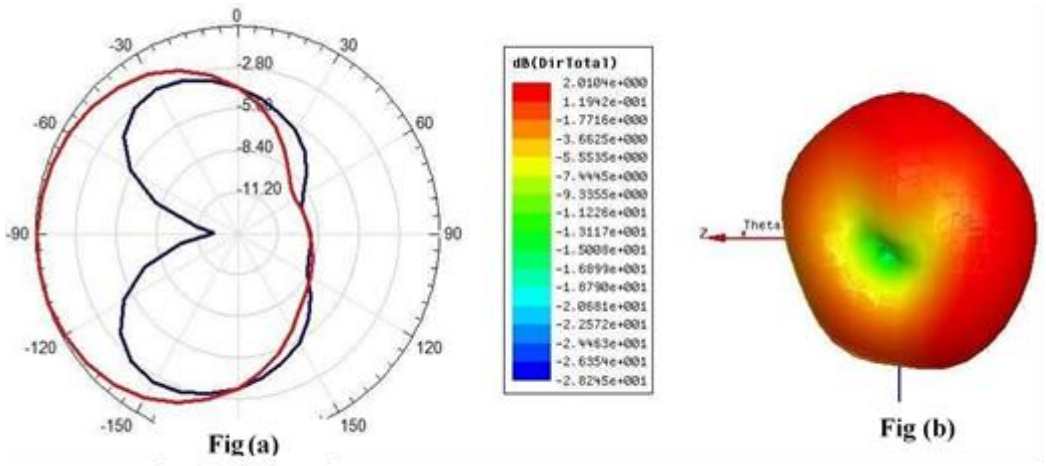

Fig 10. Simulated radiation pattern and gain of the MIMO antenna with a stub

Radiation Pattern graph (2D & 3D)

Figure 10 displays the simulated radiation pattern and gain of the MIMO antenna featuring a stub. Specifically, at a frequency of 3.5 GHz, the radiation pattern of the antenna with the stub is depicted. In subfigure (a), the antenna's radiation pattern is shown to be bi-directional in the E-plane (in blue) and omnidirectional in the H-plane (in red). Subsequently, subfigure (b) illustrates that the red color represents a peak gain of approximately 2.0 dB at 3.5 GHz. This emphasizes the directional nature of the antenna's radiation pattern and its ability to achieve significant gain at the specified frequency.

4. Simulated Results of Wideband MIMO antenna with T-Stub

3.3 Design Consideration

Figure 11 presents the layout of the suggested MIMO antenna configuration incorporating a T-stub. The top view of this MIMO diversity antenna exhibits a design consisting of a semi-circular radiator paired with a stepped partial ground plane. Notably, the diversity antenna consists of two antenna elements positioned 10 mm apart along the y-axis direction. This unique arrangement improves diversity performance, enabling effective signal reception and transmission in diverse scenarios.

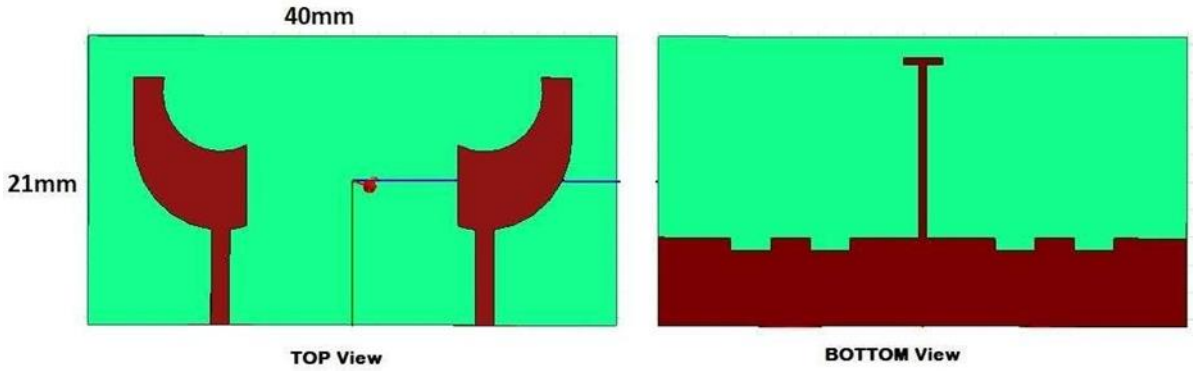

Fig 11. Wideband MIMO antenna with T-stub

4.2 Results and Discussion

4.2.1 S-Parameters graph

Figure 12 depicts the S Parameters plot of the MIMO antenna featuring a T-stub. The resonance frequency of the MIMO antenna is recorded at 5.14 GHz.

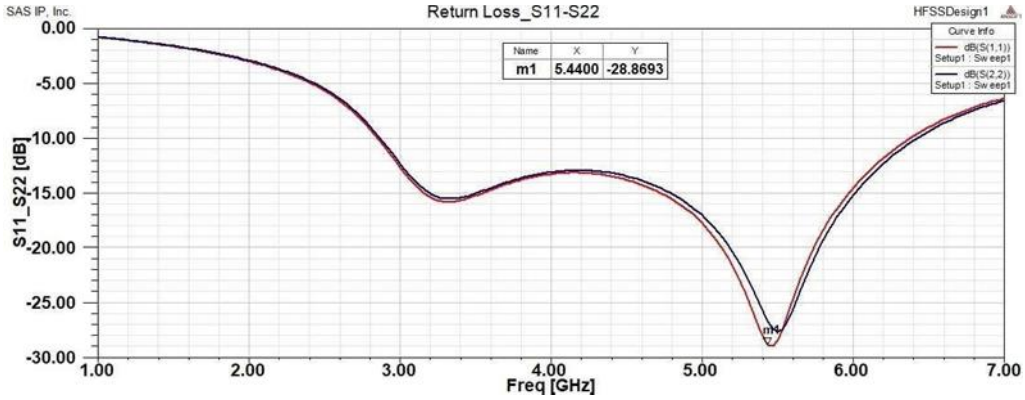

Fig 12. Simulated S-Parameters of MIMO antenna with T- stubIt can see that ReturnLoss value is -28.86at 5.44 GHz.

4.2.2 VSWR graph

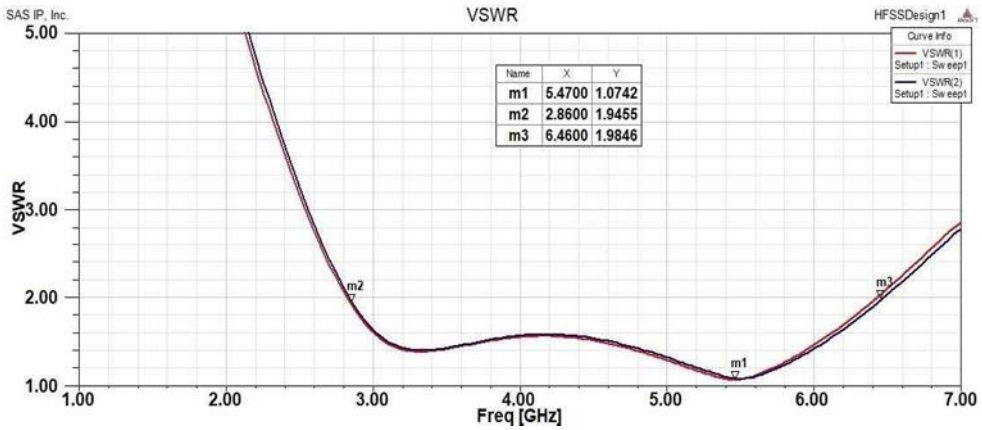

Fig 13. Simulated VSWR of MIMO antenna with T-stub

Displayed in Figure 13 is the Simulated VSWR of the MIMO antenna equipped with a T-stub, indicating that the VSWR value is 1.07 at 5.47 GHz. It can be inferred that the MIMO antenna featuring a T-stub provides an outstanding bandwidth of 3600 MHz, ranging from 2.86 GHz to 6.46 GHz.

4.2.3 Isolation Graph (S21)

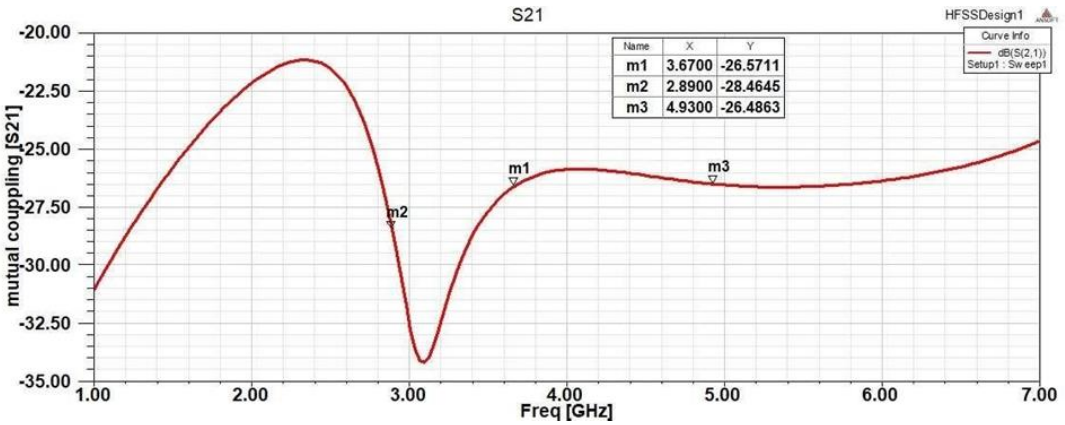

Fig 14. Isolation S21 of MIMO Antenna with T-stub

Figure 14 presents the S21 isolation plot, illustrating the performance of the MIMO antenna with a T-stub. It is clear that the isolation (S21) consistently stays below -25.00 dB across the entire operational bandwidth. This finding indicates a significant improvement in minimizing mutual coupling (S21) in the MIMO setup by incorporating the T-stub structure.

4.2.4 Radiation Pattern graph (2D & 3D)

Figure 15 displays the radiation pattern of the MIMO antenna, featuring a T-stub, at 3.5 GHz. Subfigure (a) exhibits the antenna's radiation pattern with the T-stub, showing a bi-directional pattern in the E-plane (depicted in blue) and an omnidirectional pattern in the H-plane (illustrated in red). Furthermore, subfigure (b) indicates that the red color represents a peak gain of around 2.0 dB at 3.5 GHz. This highlights the directional attributes

of the antenna's radiation pattern and its capability to achieve significant gain at the specified frequency.

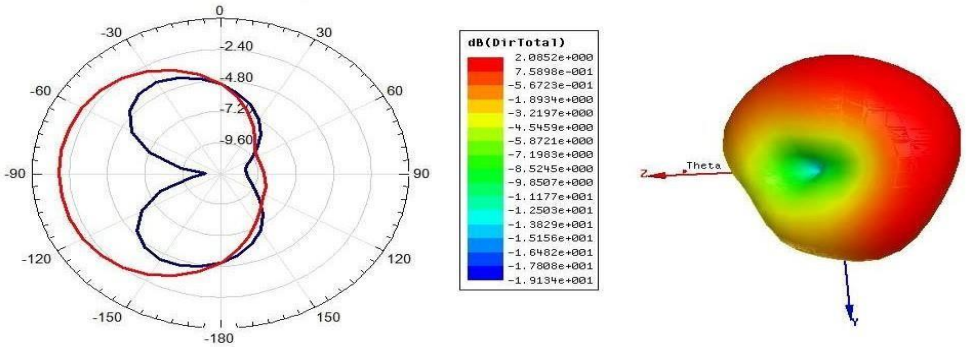

Fig (a) Fig (b)

Fig 15. Simulated Radiation pattern and gain of MIMO antenna with T- stub

Table.1 MIMO Antenna Comparison table

Sr. No.	**Results**	**S11_S22 (dB)**	**VSWR**	**BW (GHz)**	**BW (%)**	**Isolation S21 (dB)**	**Gain (dB)**	**ECC**
1.	MIMO Antenna Without Stub Results	-19.84	1.24	3.6 (2.80-6.40)	96.31	**-16.53**	2.0	0.0005
2.	MIMO Antenna With Stub Results	-29.16	1.06	3.5 (3.10-6.49)	95.31	**-23.11**	2.0	0.0005
3.	MIMO Antenna With T- Stub Results	-28.86	1.07	3.6 (2.80-6.40)	96.31	**-26.50**	2.0	0.0002

Table II Performance comparison of the MIMO with reference antennas

Ref.	Size (mm^2)	Freq (GHz)	Bandwidth [MHz]	Isolation S21 [dB]	ECC	CCL
[5]	80 x 100	2.8	100	< 20	0.3	No
[6]	32 x 57	5.8	210	< 18	0.05	No
[7]	30 x 65	2.4	90	< 14	NA	No
[8]	30 x 54	5.8	200	< 18	0.05	No
[9]	10 x 41	2.4	80	< 15	0.1	No
[10]	38 x 43	5.3	130	< 12	0.001	No
[11]	65 x 100	2.4	500	< 14	0.01	No
[12]	60 x 95	2.0	300	< 19	NA	No
[13]	30 x 38	5.0	NA	< 18	0.01	No
[14]	70 x 140	3.5	340	< 18	NA	No

5. Conclusion and Future Work

The compact MIMO antenna was meticulously crafted and simulated using HFSS software, tailored specifically for wireless applications. Through simulation, variants including the MIMO antenna without a stub, as well as configurations featuring a T-stub, were meticulously designed and evaluated. Notably, the MIMO antenna lacking a stub demonstrated an impressive isolation reaching up to -16.53 dB. Furthermore, the proposed MIMO antenna exhibited exceptional bandwidth spanning 3600 MHz (from 2.33 GHz to 5.90 GHz), accompanied by a peak gain of approximately 2.2 dB The proposed antenna has very small dimension of 21 x 40 mm2. The designed MIMO antenna covers 5G bands of, 3.3-3.8 GHz (n48/n77/n78), 4.4-5.0 GHz (n80). MIMO Antenna with T Stub got the improved isolationof -26.50 dB As the proposed antenna is of MIMO type and have a very small size, operating up to 3.3 GHz frequency, this work can be explored by hardware design of these antenna and testing them in to the real time environment. Further, size reduction also bebeneficial in the real-life-scenario.

References:

[1] P. Yang, F. Yang, and T. Dong, “Microstrip Phased Array In-band RCS Reduction with a Random Element Rotation Technique,” in *Proc. IEEE*, 2016.

[2] L. E. I. Gan, W. E. N. Jiang, Q. Chen, X. Li, and Z. Zhou, “Analysis and Reduction on In-Band RCS of Fabry-Perot Antennas,” in *Proc. IEEE*, 2020.

[3] K. W. Kim, “Wideband High-Gain Circularly-Polarized Low RCS Dipole Antenna With a Frequency Selective Surface,” *IEEE Access*, 2019.

[4] Z. A. N. K. U. I. Meng, Y. A. N. Shi, S. Member, W. E. N. Y. U. E. Wei, and X. F. A. N. Zhang, “Multifunctional Scattering Antenna Array Design for Orbital Angular Momentum Vortex Wave and RCS Reduction,” in *Proc. IEEE*, 2020.

[5] R. Mark, N. Rajak, S. Das, "Isolation Enhancement in Two Port MIMO System Using Parallel Coupled Lines," in *Proc. URSI Asia-Pacific Radio Science Conference (AP-RASC)*, 2019, pp. 1-4.

[6] Iqbal, O. A. Saraereh, A. Bouazizi, A. Basir, "Metamaterial-Based Highly Isolated MIMO Antenna for Portable Wireless Applications," Electronics, vol. 7, no. 10, pp. 1-8, 2018.

[7] S. W. Su, C. T. Lee, F. S. Chang, "Printed MIMO Antenna System Using Neutralization -Line Technique for Wireless USB-Dongle Applications," *IEEE Transactions on Antenna and Propagation*, vol. 60, no. 2, pp. 456-463, 2012.

[8] M. A. Abdalla, A. Ibrahim, "Simple μ-Negative Half Mode CRLH Antenna Configuration for MIMO Applications," *Radio engineering*, vol. 26, no. 1, pp. 45–50, 2017.

[9] J. Ryu, H. Kim, "Compact MIMO Antenna for Application to Smart Glasses using T-shaped Ground Plane," *Microwave and Optical Technology Letters*, vol. 60, no. 8, pp. 2010–13, 2018.

[10] Dkiouak, A. Zakriti, M. El. Quahabi, A. Zugari, M. Khalladi, "Design of a Compact MIMO Antenna for Wireless Applications," Progress In Electromagnetics Research M, vol. 72, pp. 115–24, 2018.

[11] Z. Yang, H. Yang, H. Cui, "A Compact MIMO Antenna with Inverted C-Shaped Ground Branches for Mobile Terminals," *International Journal of Antenna and Propagation*, vol. 2016, pp. 1-6, 2016.

[12] Z. Li, Z. Du, M. Takahashi, K. Saito, K. Ito, "Reducing Mutual Coupling of MIMO Antennas With Parasitic Elements for Mobile Terminals," *IEEE Transactions on Antennas and Propagation*, vol. 60, no. 2, pp. 473-481, 2012.

[13] S. S. Al-Bawri et al., "Broadband Sub-6GHz Slot-based MIMO Antenna for 5G NR Bands Mobile Applications," in *Proc. Journal of Physics: Conference Series, The 1st International Conference on Engineering and Technology (ICoEngTech)*, 2021, pp. 1-7.

[14] Z. Xu, C. Deng, "High-Isolated MIMO Antenna Design Based on Pattern Diversity for 5G Mobile Terminals," *IEEE Antennas and Wireless Propagation Letters*, vol. 19, no. 3, pp. 467-471, 2020.

[15] J. Li, T. A. Khan, X. Meng, J. Chen, G. Peng, and A. Zhang, “Wideband radar cross-section reduction of microstrip patch antenna using coding metasurface,” in *Proc. IEEE*, 2019.